Supplementary Information for

Electrophysiological measures from iPSC-derived neurons are associated with schizophrenia and predict donor cognitive performance

Stephanie Cerceo Page[1*], Srinidhi Rao Sripathy[1*], Federica Farinelli[1*], Zengyou Ye[1*], Yanhong Wang[1*], Daniel J Hiler[1], Elizabeth A Pattie[1], Claudia V Nguyen[1], Madhavi Tippani[1], Rebecca L. Moses[1], Huei-Ying Chen[1], Matthew Nguyen Tran[1,2], Nicholas J Eagles[1], Joshua M Stolz[1], Joseph L Catallini II[1,3], Olivia R Soudry[1], Dwight Dickinson[4], Karen F Berman[4], Jose A Apud[4], Daniel R Weinberger[1,2,5,6,7], Keri Martinowich[1,5,6#], Andrew E Jaffe[1,3,5,6,8#], Richard E Straub[1#], Brady J Maher[1,5,6#†]

Brady J. Maher
Brady.maher@libd.org

This PDF file includes:

Figures S1-S12
Index of Datasets S1 to S7

Other supplementary materials for this manuscript include the following:

Datasets S1 to S7

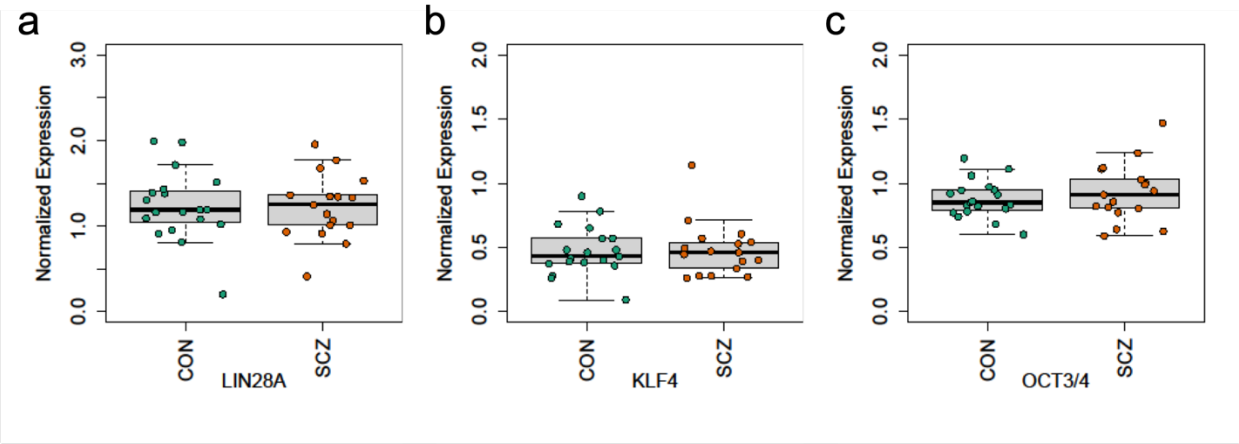

Fig. S1. No significant effect of diagnosis on hiPSC pluripotency. qPCR quantification of stem cell markers in **a,** *LIN28A* (CON=1.247 ± 0.101, SCZ=1.225 ± 0.092, p=0.87, N=35 from 28 genomes), **b,** *KLF4* (CON=0.418 ± 0.045, SCZ=0.4805 ± 0.051, p=0.37, N=35 from 28 genomes) and **c,** *OCT3/4* (CON=0.882 ± 0.033, SCZ=0.924 ± 0.055, p=0.51, N=35 from 28 genomes), all normalized to their expression in embryonic stem cell line H1.

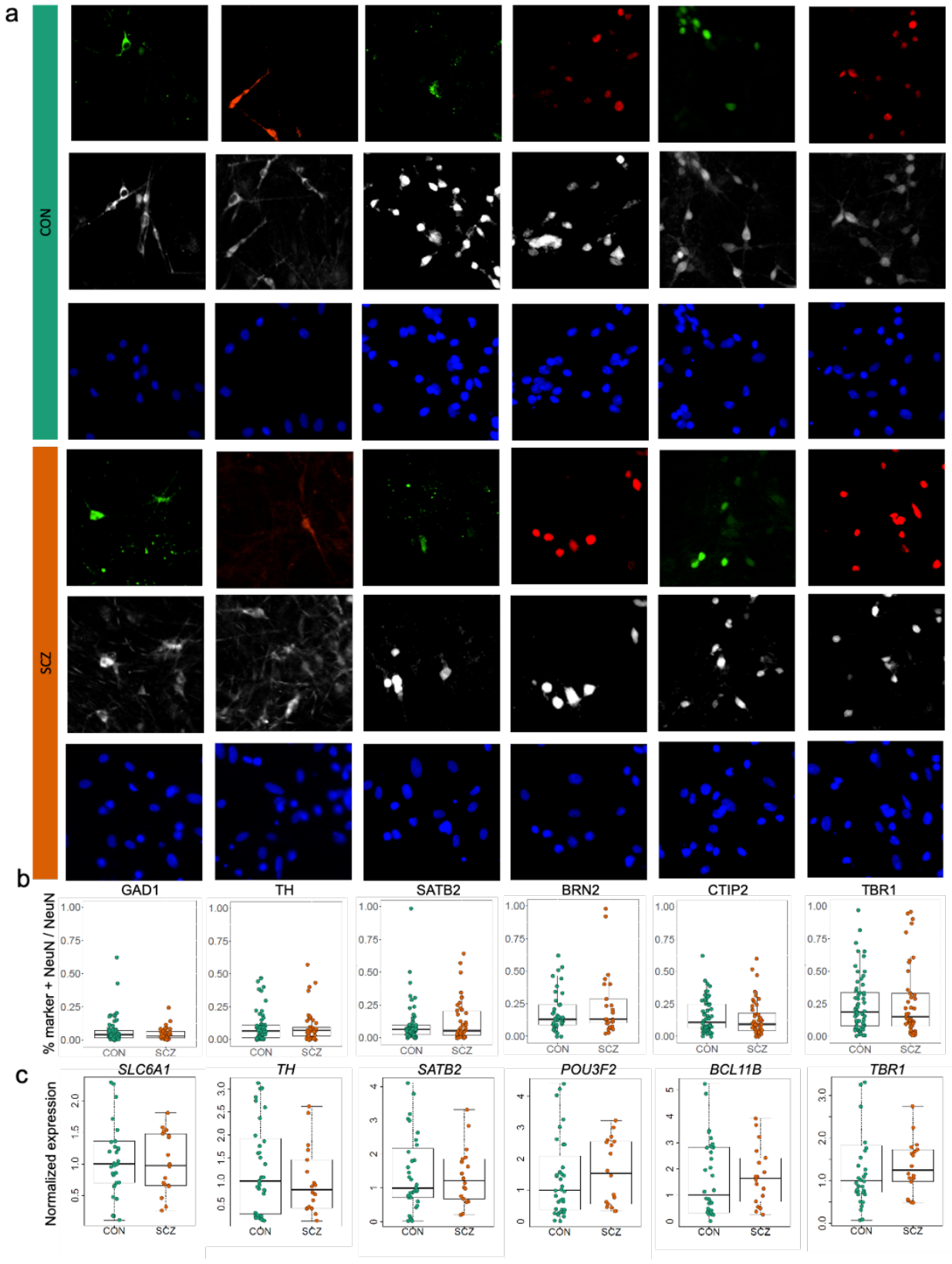
a
CON
SCZ
b
GAD1
TH
SATB2
BRN2
CTIP2
TBR1
% marker + NeuN / NeuN
1.00
0.75
0.50
0.25
0.00
CON
SCZ
c
SLC6A1
TH
SATB2
POU3F2
BCL11B
TBR1
Normalized expression

Fig. S2. Neuron cell types generated are not different by diagnosis. a, Representative image from the same line (orchid), 70 days post-differentiation, DAPI (blue), NeuN (white), and cellular identity markers GAD67 (green) and tyrosine hydroxylase (TH, red), upper cortical layer markers SATB2 (green) and BRN2 (red), and deeper cortical layers markers CTIP2 (green) and TBR1 (red). **b,** Following each differentiation, lines from each cohort were assayed for neuronal identity markers using immunocytochemistry followed by high-content imaging. We observed no differences in cell type composition between SCZ and CON lines when quantification was performed by proportion (Marker+NeuN+/NeuN+ cells: GAD1 CON=0.0643 ± 0.015, N=26; SCZ=0.0561 ± 0.013, N=32, full linear model p=0.95; TH CON=0.089 ± 0.018, N=26; SCZ=0.091 ± 0.019, N=29, full linear model p=0.92; SATB2 CON=0.141 ± 0.039, N=27; SCZ=0.107 ± 0.021, N=33, full linear model p=0.003; BRN2 CON=0.192 ± 0.035, N=21; SCZ=0.196 ± 0.040, N=25, full linear model p=0.83; CTIP2 CON=0.182 ± 0.025, N=28; SCZ=0.135 ± 0.021, N=34, full linear model p=0.49; TBR1 CON=0.237 ± 0.042, N=28; SCZ=0.315 ± 0.048, N=34, full linear model p=0.43). **c,** Normalized gene expression at DIV 70 showed no differences between CON and SCZ lines. Gene expression was normalized to mean expression of CON: *SLC6A1* (GAT1)(SCZ effect=0.98, p=0.94 N=26 across 11 genomes), *TH* (SCZ effect=0.89, p=0.78 N=27 across 11 genomes, *SATB2* (SCZ effect=1.15, p=0.76, N=27 across 11 genomes), *POU3F2* (BRN2) (SCZ effect=1.49, p=0.43, N=27 across 11 genomes), *BCL11B* (CTIP2) (SCZ effect=1.60, p=0.39, N=27 across 11 genomes), *TBR1* (SCZ effect=1.11, p= 0.78, N=27 across 11 genomes).

a
NeuN Proportion
b
BRN2 Proportion
c
CTIP2 Proportion
d
CUX1 Proportion
e
SATB2 Proportion
f
TBR1 Proportion
g
GAD Proportion
h
TH Proportion
0.0
0.2
0.4
0.6
0.8
1.0
apple
basil
butter
carrot
clay
coffee
corn
iris
mauve
mustard
orchid
plum
raisin
rust
squash
tiger
wood
yam
dijon
garnet
grape
honey
lilac
melon
mocha
pecan
pine
ruby
sage
sun
violet
yellow

Fig. S3. Summary data of immunocytochemistry of neuronal cell type and cortical layer markers for each line. a, Summary data by line for percentage of neurons by line. **b,** Summary data by line for percentage of BRN2+ neurons. **c,** Summary data by line for percentage of CTIP2+ neurons. **d,** Summary data by line for percentage of CUX1+ neurons. **e,** Summary data by line for percentage of SATB2+ neurons. **f,** Summary data by line for percentage of TBR1+ neurons. **g,** Summary data by line for percentage of GABAergic neurons. **h,** Summary data by line for percentage of TH+ neurons.

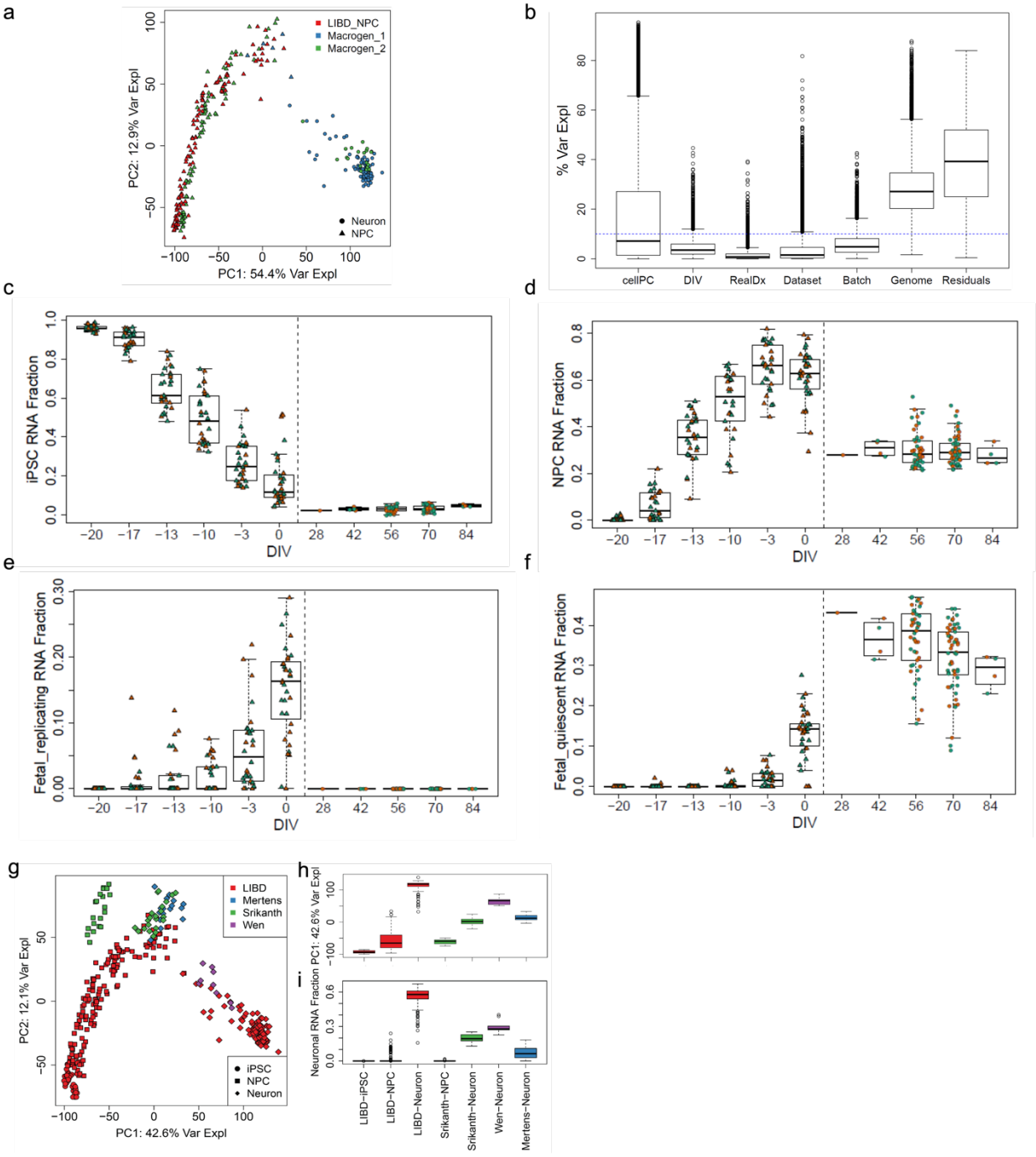
a
LIBD_NPC
Macrogen_1
Macrogen_2
Neuron
NPC
PC1: 54.4% Var Expl
PC2: 12.9% Var Expl
b
% Var Expl
cellPC
DIV
RealDx
Dataset
Batch
Genome
Residuals
c
iPSC RNA Fraction
DIV
d
NPC RNA Fraction
DIV
e
Fetal_replicating RNA Fraction
DIV
f
Fetal_quiescent RNA Fraction
DIV
g
LIBD
Mertens
Srikanth
Wen
iPSC
NPC
Neuron
PC1: 42.6% Var Expl
PC2: 12.1% Var Expl
h
PC1: 42.6% Var Expl
i
Neuronal RNA Fraction
LIBD−iPSC
LIBD−NPC
LIBD−Neuron
Srikanth−NPC
Srikanth−Neuron
Wen−Neuron
Mertens−Neuron

Fig. S4. RNA-seq validation of cell states. a, Top principal components of gene expression relate to developmental changes. Triangle = NPC, Circle = Neuron; Color = batch. **b,** Variance components analyses of gene expression across each gene (ie each box is the distribution of variance explained across all expressed genes) - developmental stage and genome strongly influence expression variation, while differentiation round or the individual performing the differentiation did not. **c,** We represented cellular heterogeneity as the first principal component of the 10 cell class fractions, which captured 84% of the cellular variance explained, where adult and fetal quiescent neuron RNA fractions were associated with increased maturity, and NPCs and endothelial RNA fractions were associated with decreased maturity. As expected, hiPSC RNA signature decreases over development. **d,** The RNA fraction associated with NPCs increases then decreases over development. **e,** We used RNA deconvolution to estimate the RNA fractions for multiple cell classes, and confirmed that our cells align with the fetal-replicating class during the hNPC stage. **f,** Neurons display the fetal-quiescent class during the post-mitotic neuronal stage. **g,** Principal component analysis (PCA) performed on the human gene expression levels generated in this manuscript (in red, "LIBD"), visualizing PC1 versus PC2, the largest two components of variation. Point shapes corresponding to cell state (iPSC, NPC, and neuron). Identically-processed public datasets (other point colors) were projected into this latent space (PC1 versus PC2) and overlaid in the plot. **h,** Boxplot demonstrating components of variation for PC1 and **i,** the RNA fraction corresponding to the adult neuron signature, with LIBD-Neuron showing the highest degree of maturation.

a

Symbol	logFC	P.Value	Symbol	logFC	P.Value
PCDHA5	1.163113	1.85E-13	PCDHA6	-1.17762	1.29E-06
SLITRK2	2.167899	8.17E-08	ZNF439	-1.19333	2.28E-06
RP11-706O15.5	3.571087	4.23E-07	KIF17	-0.44093	3.15E-06
BMS1P1	0.544607	3.70E-06	FAM213A	-0.21657	6.07E-06
LINC01515	1.247371	2.53E-06	QPCT	-0.96649	6.55E-06
WNT8B	1.950148	9.36E-06	CYP4V2	-0.37801	1.25E-05
RP11-403I13.4	2.444786	2.45E-06	HLA-C	-0.79398	1.37E-05
RP11-274B21.13	0.379279	3.52E-05	EIF3FP3	-0.32375	1.97E-05
PLAGL1	0.642294	6.23E-05	PIGP	-0.35342	2.35E-05
ALG1L	1.604253	2.42E-05	PLOD1	-0.38	2.35E-05
RP11-989F5.3	0.974478	2.77E-05	HIST1H4H	-0.46269	2.29E-05
FRG1HP	0.355813	7.90E-05	AC020951.1	-1.56885	1.38E-05
NOVA1	0.416503	6.58E-05	SLC22A18	-0.65611	2.90E-05
MASP1	1.176606	9.65E-05	AC004381.6	-0.34403	4.00E-05
FEZF2	1.379008	9.18E-05	LGI4	-0.46152	4.82E-05
RP11-398E10.1	1.344732	4.27E-05	CHURC1	-0.30646	5.15E-05
ZNF560	1.504064	1.06E-04	AGGF1P2	-2.01103	9.86E-06
MDGA2	1.122355	1.06E-04	FAM118A	-0.41141	8.46E-05
PAPPA	0.552511	1.62E-04	AGGF1P1	-1.75729	1.81E-05
SPTLC3	1.015732	1.81E-04	RWDD2B	-0.98266	1.28E-04
SLC15A2	0.824088	1.98E-04	KRT19	-0.86901	1.13E-04
TTC3	0.141323	1.34E-04	BTN3A2	-0.68788	1.59E-04
ALDH1A1	1.715567	1.45E-04	SFRP1	-0.4807	1.62E-04
			COL18A1	-0.49178	1.63E-04

b

- Increased in SCZD:
  - Frizzled binding (p = 9.3e-8)
  - Cell fate commitment (p=4.4e-7)
  - forebrain regionalization (p=1.6e-5)
  - Canonical Wnt signaling (p=7.6e-5)
  - Hippo signaling (p=9.9e-4)

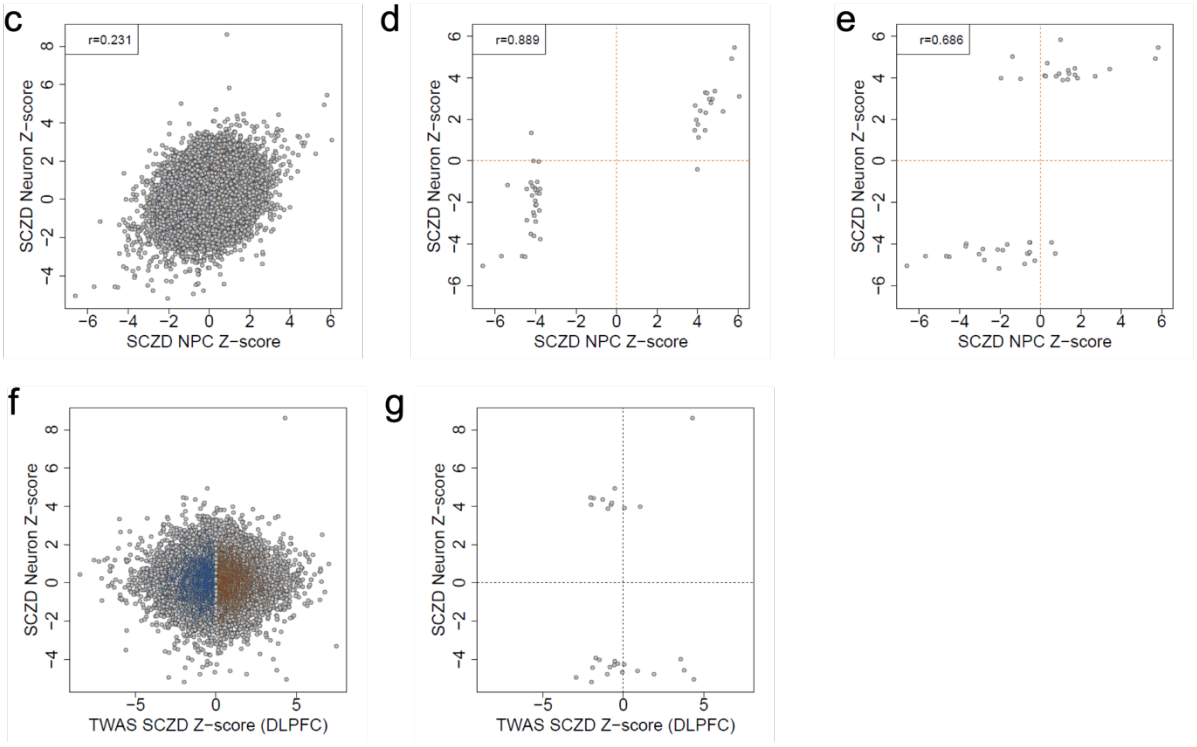

Fig. S5. Gene expression changes in hiPSC-derived neurons correlate across cell states. **a,** Differentially expressed genes with FDR<0.05. **b,** Representative GO terms from DEGs at p<0.005. **c,** Gene expression correlates across cell states. **d,** Differentially expressed genes in neurons are observed in NPCs. **e,** Genes that are differentially expressed in NPCs remain differentially expressed in neurons. **f,** Correlation between gene expression in hiPSC-derived neurons when compared to TWAS data from postmortem DLPFC. **g,** Differential expression in hiPSC-derived neurons compared to TWAS data.

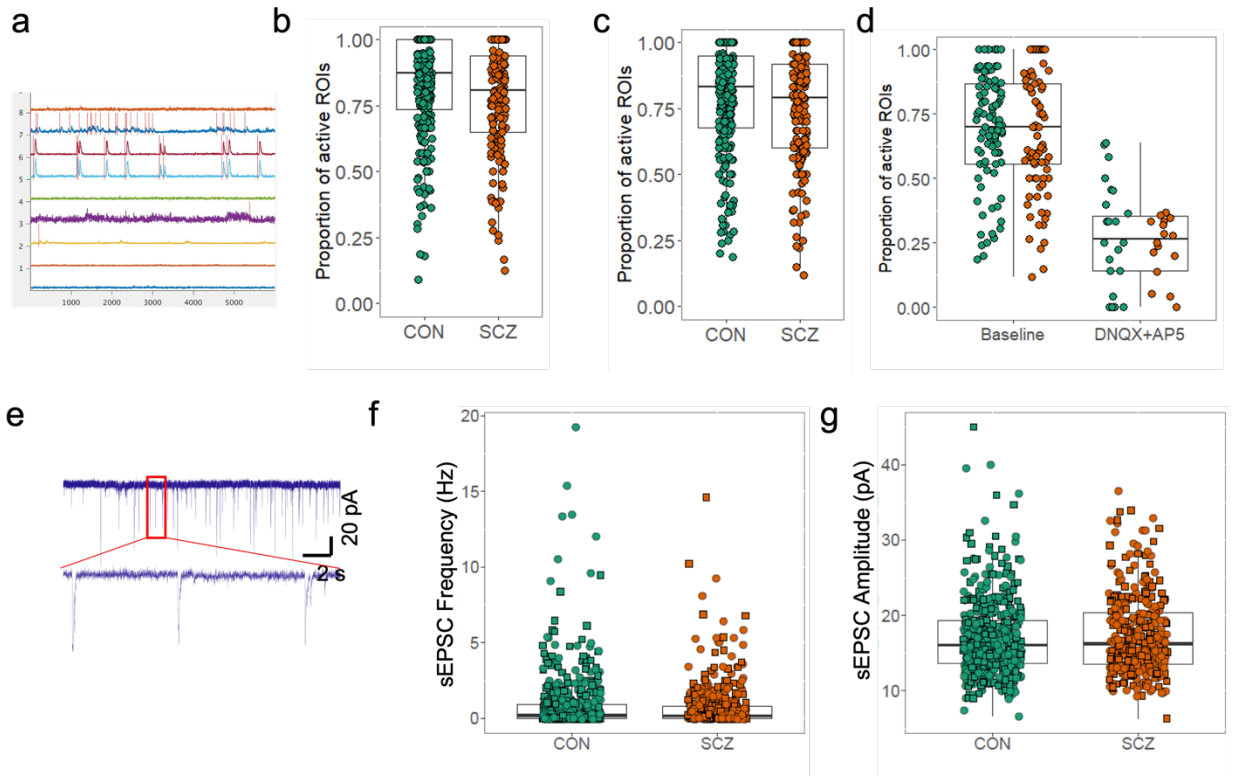

Fig. S6. Physiological assessment of cortical neurons. a, Representative traces of regions of interest in a CONculture. **b,** Proportion of active ROIs are not significantly different between CON and SCZ at an early developmental stage (DIV42, SCZ effect= -0.0494, p=0.403, N=426 across 35 lines). **c,** Proportion of active ROIs are not significantly different at a later developmental stage (DIV63) between CON and SCZ(SCZ effect= -0.0381, p=0.542, N=419 across 35 lines). **d,** Spontaneous network activity was primarily driven by glutamatergic synaptic transmission as the application of glutamatergic inhibitors dl-AP5 (100μM) and DNQX (10μM) results in a 70.2% decrease in the percentage of active ROIs in both CON and SCZ lines (N=14 CON, 8 SCZ lines, p=2.15E-22). **e,** Representative traces of spontaneous excitatory postsynaptic currents. **f,** Frequency of sEPSCs are not significantly different between CON and SCZ (SCZ effect=-0.147, p=0.188, N=954 across 28 genomes). **g,** Amplitude of sEPSCs are not significantly different between CON and SCZ (SCZ effect=0.294, p=0.408, N=806 across 28 genomes).

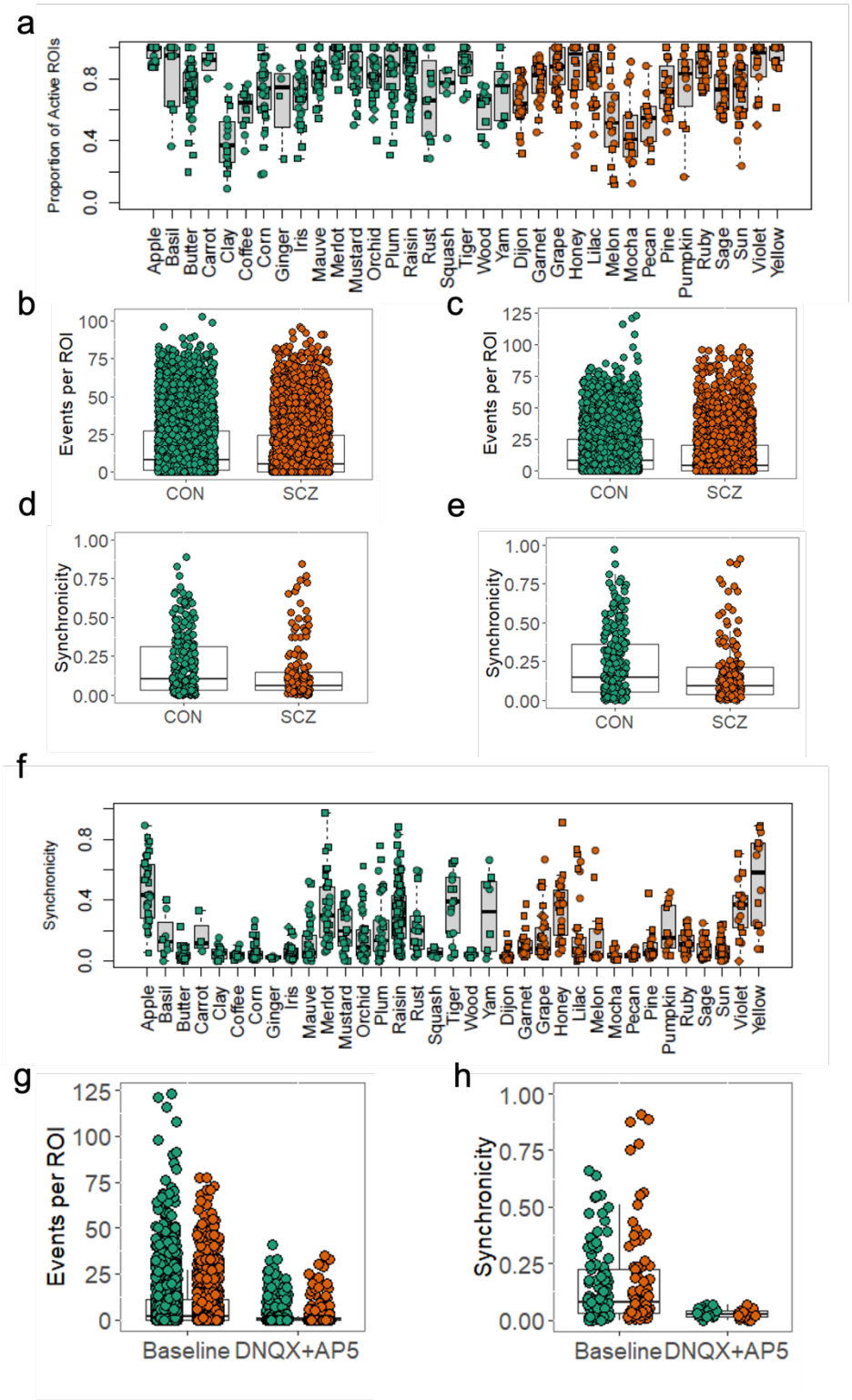
a
Proportion of Active ROIs
0.0
0.4
0.8
Apple
Basil
Butter
Carrot
Clay
Coffee
Corn
Ginger
Iris
Mauve
Merlot
Mustard
Orchid
Plum
Raisin
Rust
Squash
Tiger
Wood
Yam
Dijon
Garnet
Grape
Honey
Lilac
Melon
Mocha
Pecan
Pine
Pumpkin
Ruby
Sage
Sun
Violet
Yellow
b
Events per ROI
0
25
50
75
100
CON
SCZ
c
Events per ROI
0
25
50
75
100
125
CON
SCZ
d
Synchronicity
0.00
0.25
0.50
0.75
1.00
CON
SCZ
e
Synchronicity
0.00
0.25
0.50
0.75
1.00
CON
SCZ
f
Synchronicity
0.0
0.4
0.8
Apple
Basil
Butter
Carrot
Clay
Coffee
Corn
Ginger
Iris
Mauve
Merlot
Mustard
Orchid
Plum
Raisin
Rust
Squash
Tiger
Wood
Yam
Dijon
Garnet
Grape
Honey
Lilac
Melon
Mocha
Pecan
Pine
Pumpkin
Ruby
Sage
Sun
Violet
Yellow
g
Events per ROI
0
25
50
75
100
125
Baseline
DNQX+AP5
h
Synchronicity
0.00
0.25
0.50
0.75
1.00
Baseline
DNQX+AP5

Fig. S7. Summary data of calcium imaging by diagnosis and by line. a, Proportion of active ROIs by line (circle DIV42, square DIV63). **b,** Summary data of events per ROI by diagnosis at DIV42 (SCZ effect= -0.0136, p=0.9414, N_{CON}=3902, N_{SCZ}=2927). **c,** Summary data of events per ROI by diagnosis at DIV63 (SCZ effect=-0.040, p=0.828 N_{CON}=3616, N_{SCZ}=2866) **d,** Summary data of synchronicity of events by diagnosis at DIV42 (SCZ effect=-0.00383, p=0.9428, N_{CON}=3902, N_{SCZ}=2927). **e,** Summary data of synchronicity by diagnosis at DIV63 (SCZ effect=-0.0165, p=0.761, N_{CON}=3616, N_{SCZ}=2866). **f,** Synchronicity by line. **g,** Number of events per ROI is reduced following application of DNQX (10μM) and dl-AP5 (100μM), (baseline: N=2842, 8.37 ± 0.257, DNQX + AP5: N=739, 2.14 ± 0.204, p=1.34E-6) **h,** Synchronicity of events is decreased following application of DNQX (10μM) and dl-AP5 (100μM), (baseline: N=177, 0.160 ± 0.012, DNQX + AP5: N=38, 0.029 ± 0.00489, p=3.7E-5).

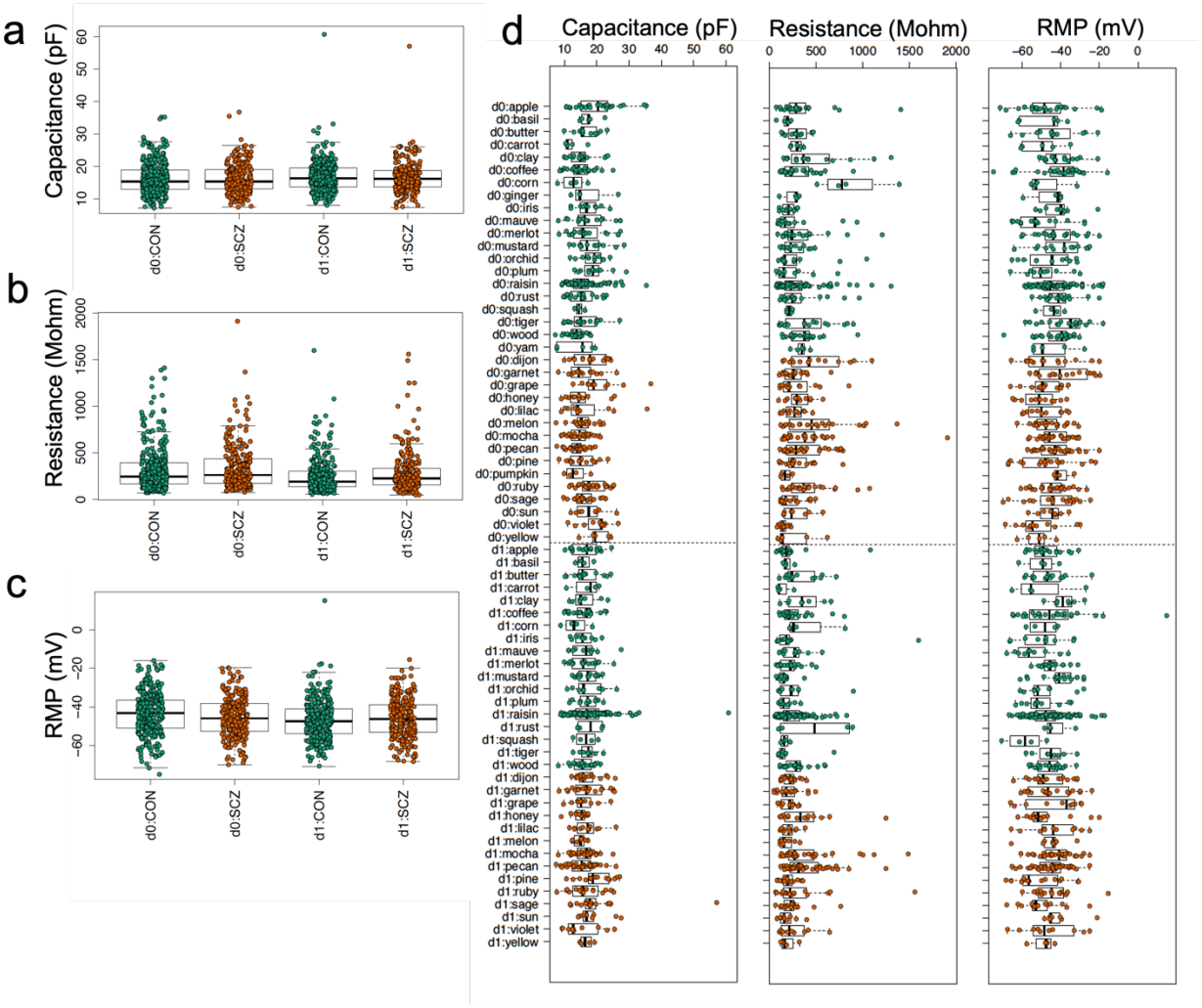
a
Capacitance (pF)
10
20
30
40
50
60
d0:CON
d0:SCZ
d1:CON
d1:SCZ
b
Resistance (Mohm)
0
500
1000
1500
2000
c
RMP (mV)
0
−20
−40
−60
d
Capacitance (pF)
Resistance (Mohm)
RMP (mV)
−60
−40
−20
d0:apple
d0:basil
d0:butter
d0:carrot
d0:clay
d0:coffee
d0:corn
d0:ginger
d0:iris
d0:mauve
d0:merlot
d0:mustard
d0:orchid
d0:plum
d0:raisin
d0:rust
d0:squash
d0:tiger
d0:wood
d0:yam
d0:dijon
d0:garnet
d0:grape
d0:honey
d0:lilac
d0:melon
d0:mocha
d0:pecan
d0:pine
d0:pumpkin
d0:ruby
d0:sage
d0:sun
d0:violet
d0:yellow
d1:apple
d1:basil
d1:butter
d1:carrot
d1:clay
d1:coffee
d1:corn
d1:iris
d1:mauve
d1:merlot
d1:mustard
d1:orchid
d1:plum
d1:raisin
d1:rust
d1:squash
d1:tiger
d1:wood
d1:dijon
d1:garnet
d1:grape
d1:honey
d1:lilac
d1:melon
d1:mocha
d1:pecan
d1:pine
d1:ruby
d1:sage
d1:sun
d1:violet
d1:yellow

Fig. S8. Neuronal maturation of membrane properties. a, Summary data by diagnosis showing membrane capacitance increases between DIV 56 (d0) and 70 (d1)(d1-d0 effect=0.799, p=0.003, N=1086), but is not different by diagnosis (Both timepoints SCZ effect=-0.043, p=0.878, N=1086; d0 SCZ effect=0.064, p=0.862, N=566 across 28 genomes; d1 SCZ effect=-0.182, p=0.666, N=520 across 28 genomes). **b,** Group data showing membrane resistance increases between DIV 57 (d0) and 70 (d1)(d1-d0 effect=-55.11, p=2.55E-05, N=1086), and is different by diagnosis (Both timepoints SCZ effect=29.41, p=0.026, N=1086; d0 SCZ effect=21.85, p=0.260, N=566 across 28 genomes; d1 SCZ effect=40.67, p=0.02, N=520 across 28 genomes). **c,** Summary data showing resting membrane potentials become more depolarized between DIV 57 (d0) and 70 (d1)(d1-d0 effect=-1.94, p=0.002, N=1086), but do not differ by diagnosis (Both timepoints SCZ effect=-0.665, p=0.295, N=1082; d0 SCZ effect=-2.022, p=0.023, N=565 across 28 genomes; d1 SCZ effect=0.890, p=0.331, N=517 across 28 genomes). **d,** Membrane property measures by line.

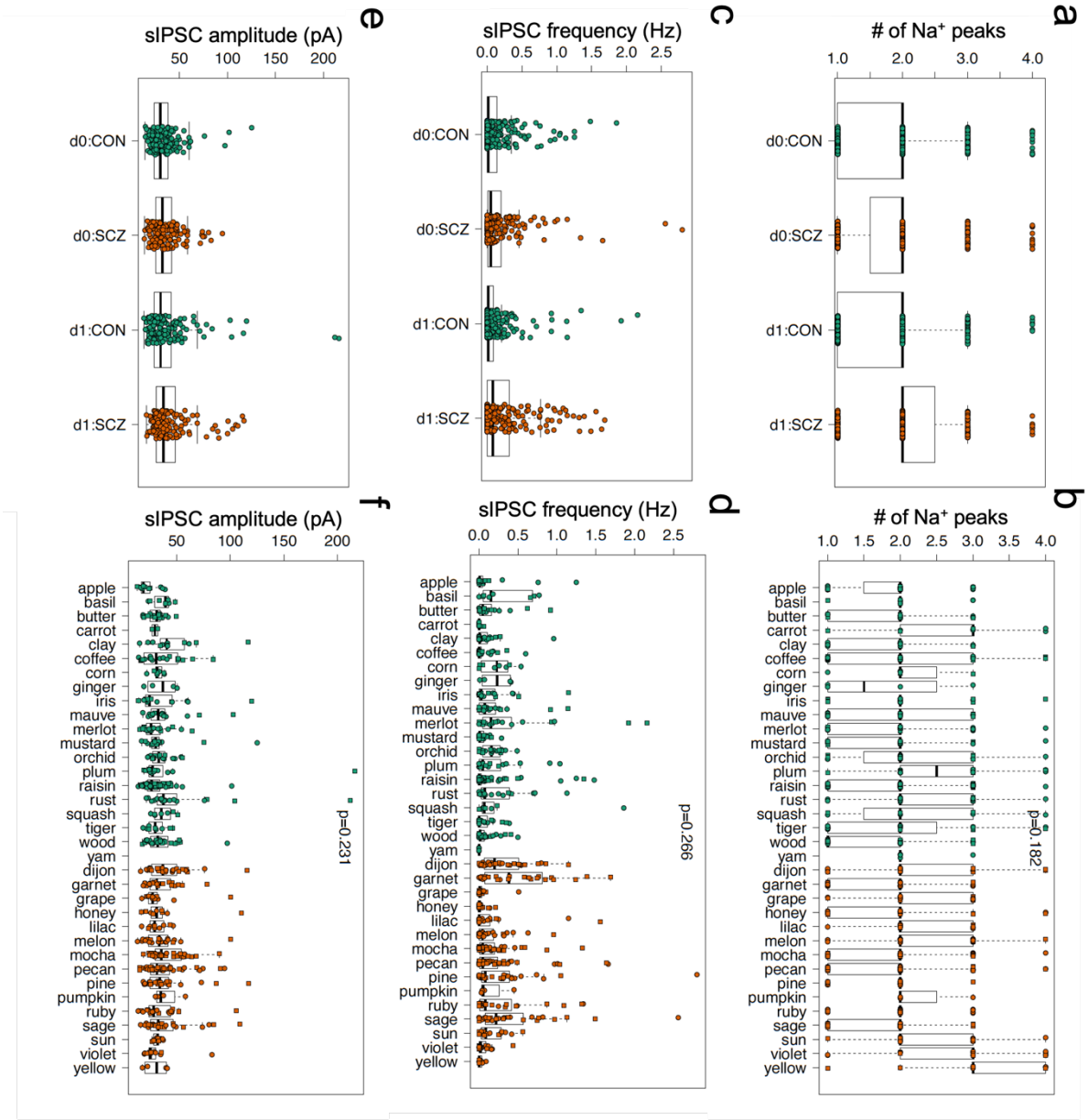
e
sIPSC amplitude (pA)
50
100
150
200
d0:CON
d0:SCZ
d1:CON
d1:SCZ
c
sIPSC frequency (Hz)
0.0
0.5
1.0
1.5
2.0
2.5
d0:CON
d0:SCZ
d1:CON
d1:SCZ
a
# of Na⁺ peaks
1.0
2.0
3.0
4.0
d0:CON
d0:SCZ
d1:CON
d1:SCZ
f
sIPSC amplitude (pA)
50
100
150
200
p=0.231
apple
basil
butter
carrot
clay
coffee
corn
ginger
iris
mauve
merlot
mustard
orchid
plum
raisin
rust
squash
tiger
wood
yam
dijon
garnet
grape
honey
lilac
melon
mocha
pecan
pine
pumpkin
ruby
sage
sun
violet
yellow
d
sIPSC frequency (Hz)
0.0
0.5
1.0
1.5
2.0
2.5
p=0.266
apple
basil
butter
carrot
clay
coffee
corn
ginger
iris
mauve
merlot
mustard
orchid
plum
raisin
rust
squash
tiger
wood
yam
dijon
garnet
grape
honey
lilac
melon
mocha
pecan
pine
pumpkin
ruby
sage
sun
violet
yellow
b
# of Na⁺ peaks
1.0
1.5
2.0
2.5
3.0
3.5
4.0
p=0.182
apple
basil
butter
carrot
clay
coffee
corn
ginger
iris
mauve
merlot
mustard
orchid
plum
raisin
rust
squash
tiger
wood
yam
dijon
garnet
grape
honey
lilac
melon
mocha
pecan
pine
pumpkin
ruby
sage
sun
violet
yellow

Fig. S9. Summary data of number of Na^+ peaks and sIPSC frequency and amplitude. a, Summary data by diagnosis showing number of Na^+ peaks for DIV 56 (d0) and 70 (d1)(Both timepoints SCZ effect=0.093, p=0.038, N=1074 across 28 genomes; d0 SCZ effect=0.043, p=0.492, N=560 across 28 genomes; d1 SCZ effect=0.146, p=0.018, N=514 across 28 genomes). **b,** Summary data of Na^+ peak counts for each line. **c,** Summary data by diagnosis showing sIPSC frequency for DIV 56 (d0) and 70 (d1)(Both timepoints SCZ effect=0.097, p=1.11E-06, N=903 across 28 genomes; d0 SCZ effect=0.049, p=0.082, N=449 across 28 genomes; d1 SCZ effect=0.143, p=2.10E-07, N=454 across 28 genomes). **d,** Summary data of sIPSC frequency for each line. **e,** Summary data by diagnosis showing sIPSC amplitude for DIV 56 (d0) and 70 (d1)(Both timepoints SCZ effect=2.131, p=10.184, N=591 across 28 genomes; d0 SCZ effect=1.903, p=0.250, N=304 across 28 genomes; d1 SCZ effect=2.421, p=0.350, N=287 across 28 genomes). **f,** Summary data of sIPSC amplitude for each line.

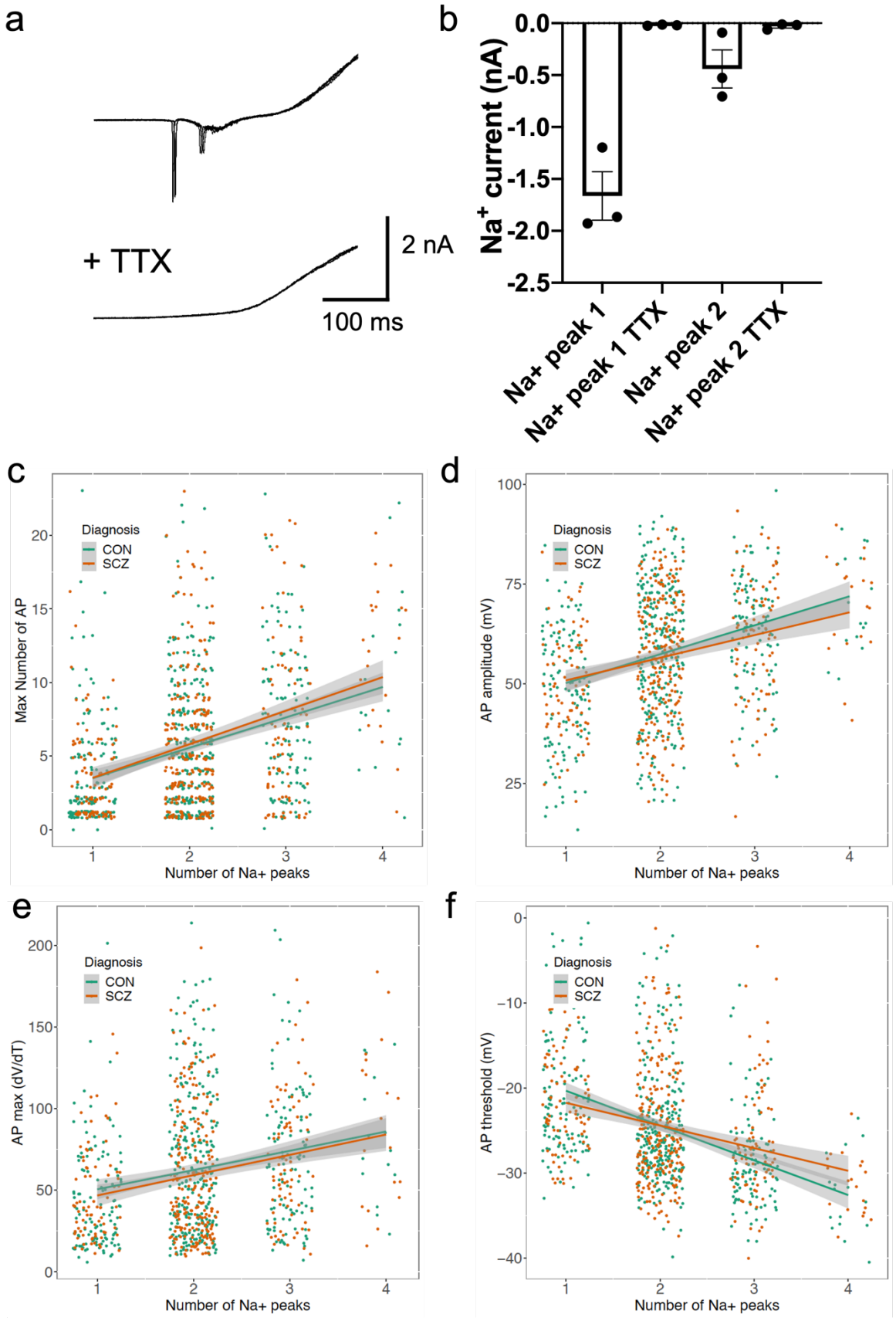
a
+ TTX
2 nA
100 ms
b
Na+ current (nA)
0.0
-0.5
-1.0
-1.5
-2.0
-2.5
Na+ peak 1
Na+ peak 1 TTX
Na+ peak 2
Na+ peak 2 TTX
c
Diagnosis
CON
SCZ
Max Number of AP
Number of Na+ peaks
d
AP amplitude (mV)
Number of Na+ peaks
e
AP max (dV/dT)
Number of Na+ peaks
f
AP threshold (mV)
Number of Na+ peaks

Fig. S10. Physiological relevance of multiple Na^+ peaks. a, Representative traces showing TTX blockade of Na^+ currents in response to a voltage ramp. **b,** Group data showing TTX blockade of Na^+ currents (peak 1 TTX effect=0.989, peak 2 TTX effect= 0.931, P_{anova}=0.015, N=3). **c,** The maximum number of action potential is correlated with the number of Na^+ peaks (CON N=625, R=0.347, p=1.87E-18; SCZ N=461, R=0.362, p=2.44E-15). **d,** The amplitude of action potentials are correlated with the number of Na^+ current peaks (CON N=625, R=0.34, p=1.78E-15; SCZ N=461, R=0.279, p=1.65E-08). **e,** The acceleration of the action potential upslope (dV/dT) is correlated with the number of Na^+ peaks (CON N=625, R=0.226, p=2.23E-07; SCZ N=461, R=0.245, p=7.89E-07). **f,** The action potential threshold is negatively correlated with the number of Na^+ peaks (CON N=625, R=-0.430, p=1.67E-24; SCZ N=461, R=-0.296, p=2.00E-09).

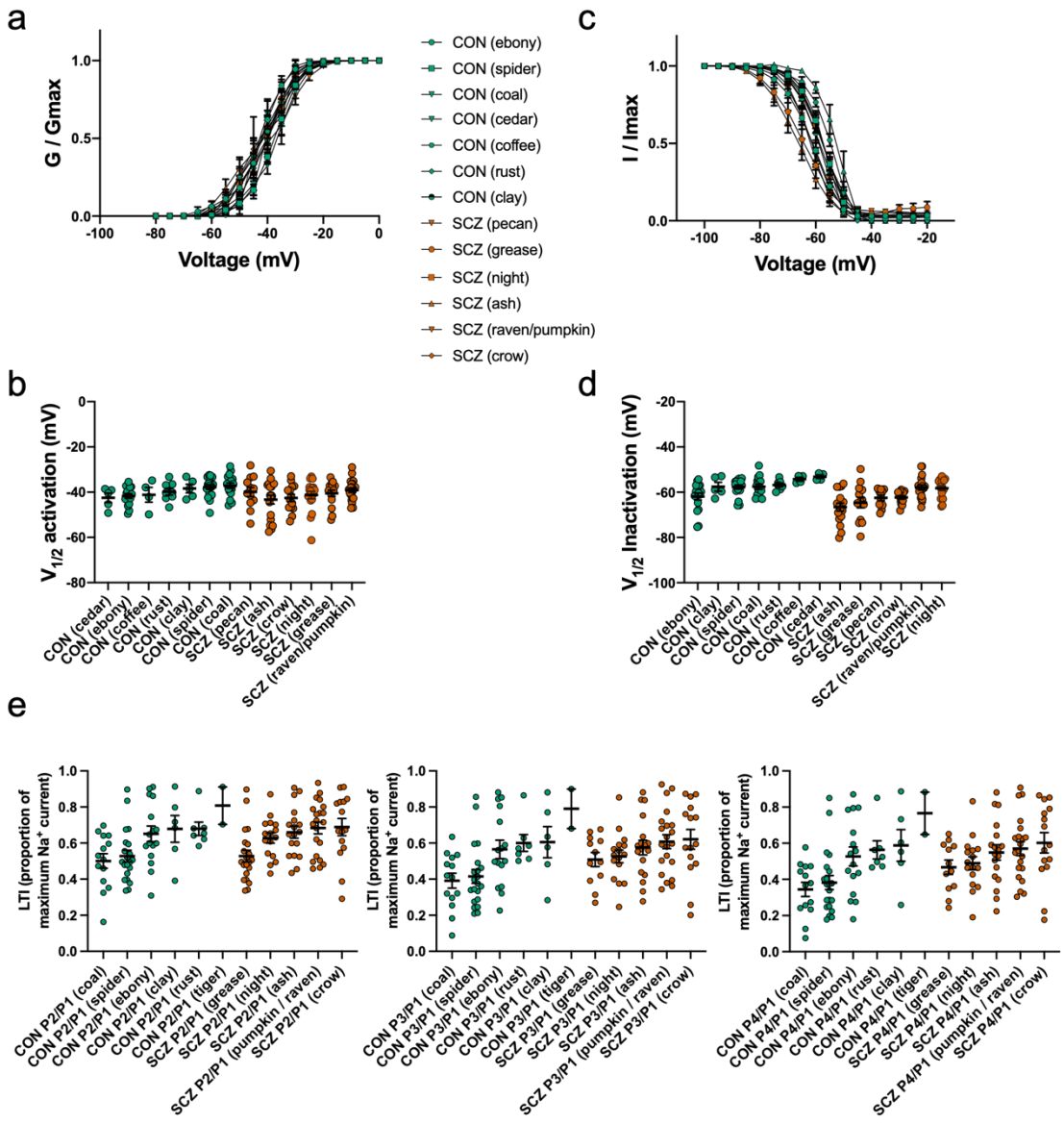

Fig. S11. Summary data for Na^+ channel activation and inactivation by genome. a, Normalized conductance versus voltage plots for 6 SCZ and 7 CON lines. **b,** Curves in (a) were fitted with a Boltzmann function and the V1/2 for each neuron is reported. **c,** Normalized inactivation versus voltage plots for 6 SCZ and 7 CON lines. **d,** Curves in (c) were fitted with a Boltzmann function and the V1/2 for inactivation for each neuron is reported. **e,** Proportion of current remaining from the first voltage step pulse after consecutive voltage step pulses (P2/P1, P3/P1, P4/P1) for each neuron is reported.

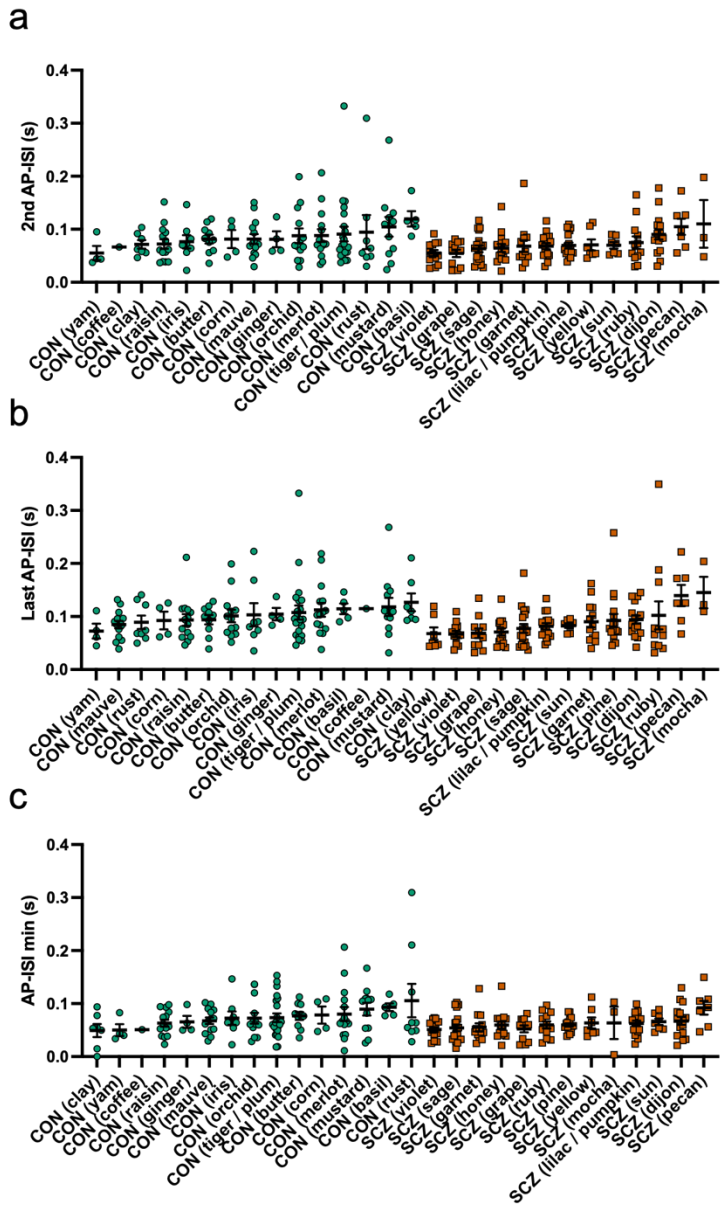

Fig. S12. Summary data of inter-spike intervals for action potentials by genome. a, Duration of the 2nd inter-spike interval for each neuron is reported. **b,** Duration of the last inter-spike interval for each neuron is reported**. c,** Duration of the minimum inter-spike interval for each neuron is reported.

Index of Datasets S1-S7